



## **EVALUATION OF SOIL LOSS AND SEDIMENT YIELD SPATIAL ASSESSMENT THROUGH GIS-BASED EMPIRICAL METHODS. A CASE STUDY OF ATALANTI CATCHMENT IN CENTRAL GREECE**

**<sup>1</sup>Lappas I.,**

<sup>1</sup>Dr. Hydrogeologist, Special Secretariat for Water, Department of Protection and Management of Aquatic Environment, Division of Surface and Ground Waters, Amaliados 17 Str., Ambelokipi-Athens, P.C. 11523<sup>2</sup>  
Kallioras A.

<sup>2</sup>Assistant Professor, National and Technical University of Athens, School of Mining and Metallurgical Engineering, Laboratory of Engineering Geology and Hydrogeology, Heron Polytechniou 9 Str., Zografou-Athens, P.C. 15780

### **Abstract**

The objective aim of this study was to estimate potential soil loss and sediment yield spatial distribution by implementing the empirical and semi-quantitative Revised Universal Soil Loss Equation (RUSLE) and Erosion Potential Method (EPM), known as Gavrilovic method, via implementation of Geographical Information System (GIS) in Atalanti river basin in Central Greece where soil erosion is quite significant. Soil erosion has been recognized to be a serious environmental and soil degradation problem arising from deforestation, agricultural intensity, over cultivation and other anthropogenic activities may lead to severe soil erosion. The current analysis refers to the erosion intensity indicating the areas the most susceptible to erosion by predicting the long-term average annual soil loss and sediment yield per unit area of the river basin by creating soil erosion maps. Also, such modelling can offer a quantitative estimation of soil erosion and sediment yield under different conditions. Both RUSLE and EPM factors and coefficients were computed by using information concerning interpolation of temperature and rainfall data, soil map (pedology), geological features, vegetation cover, digital elevation model (spatial resolution of 25 m), topographical map (slope), conservation practices based on land use (CORINE), basin physical characteristics as well as support practice factors. The parameter values were assigned to each cell and annual soil loss estimation was generated on a cell by cell basis by overlaying the derived factor maps presenting the spatial distribution of soil erosion. The calculation of the sediment delivery ratio was then applied to determine the average annual sediment yield from soil loss data. The results in the study area indicated that the rate of soil loss and sediment yield ranged from null (valley-low slope gradient areas) to extremely high. The higher soil loss-sediment yield values can be found at the hilly and mountainous areas of Atalanti region where steep and abrupt slopes prevail ( $>30^\circ$ ). On the contrary, the lower one values can be found at the central and eastern part of the study area due to the flat relief. The spatial erosion maps derived from RUSLE and EPM methods via GIS performed quite satisfactory visualization-identification of the regions prone to erosion processes and serve as an essential tool for the adoption of proper environmental monitoring, soil conservation practices, land planning and management mainly in the mountainous areas to reduce the potential soil erosion and prevent further soil degradation.

*Keywords: potential soil erosion mapping; RUSLE-EPM methods; GIS; soil conservation management; river basin*

### **1. Introduction**

Soil erosion has currently become one of the main environmental problems for soil degradation especially in mountainous areas with steeper slopes and more intense rainfall. This phenomenon varies both temporally and spatially depending on the basin's descriptive aspects (catchment morphology), the drainage network and soil characteristics, the local climate conditions, the wildfires, the land use (e.g., sparse vegetation) and management practices leading to soil fertility decline and a threat to long-term agricultural sustainability due to loss of nutrient rich surface soil and increased sediment runoff (agriculture productivity regression). Also, certain human-induced activities such as infrastructure, urbanization, mining, inappropriate agricultural management practices, deforestation, overgrazing, overcultivation, land abandonment etc. accelerate the phenomenon processes making it even more difficult to recover. Erosion is mainly triggered by a combination of factors such as climate with long dry periods followed by heavy erosive rainfall, runoff



events due to the abrupt relief, inappropriate land use and land cover patterns. Agricultural lands without vegetation cover are more vulnerable to erosion threats. The erosion models coupled with Digital Elevation Model (DEM) along with Geographical Information System (GIS) have been proved to be an effective tool for estimating and quantitatively assessing the magnitude and spatial distribution of erosion so that effective management strategies as well as soil conservation programmes can be developed and applied on a regional basis with the help of field measurements. Several methods for erosion intensity and associated sediment yield assessment have been developed categorized into empirical, conceptual and physically based models with varying accuracy and complexity. The two of the most scientifically accepted and widely applied empirical based models which estimate long-term average annual soil loss and sediment yield by sheet and rill erosion are the Revised Universal Soil Loss Equation (RUSLE) (Wischmeier et al. 1978, Renard et al. 1997) and Erosion Potential Model (EPM) (Gavrilovic 1988) predicting the erosion potential on a cell-by-cell basis in regions where measurements are completely absent. These empirical models are worldwide applied due to the ease of use, the low input data requirements, the simplicity, the computation demands, the time-consuming and the low implementation costs as well. The utmost objective of this study was to spatially assess the annual soil erosion rate and develop a soil erosion map for the three sub-catchments of Atalanti river basin in Central Greece, namely Alarginos, Karagkiozis and Ag. Ioannis by using erosion models and GIS techniques. RUSLE is an erosion estimation model by overland flow comprising six factors, namely, rain erosivity (R), soil erodibility (K), slope length (L), slope steepness (S), vegetation cover (C) and support practice actions (P) estimating the long-term average annual erosion rate also determining the catchment sediment yield by using the concept of sediment delivery ratio (SDR). The EPM model is a factor-based one such as geology and soil properties (erodibility factor), topographic features (mean slope), climate factors (mean annual rainfall and temperature), land use type and distribution (soil protection factor) and the catchment's degree of erosion which means that a series of factors, each quantifying one or more processes and their interactions are combined to yield an overall estimation of the mean annual volumes of soil erosion and sediment yield at a basin scale. Consequently, mapping soil erosion with empirical models along with GIS techniques allows identifying areas susceptible to high erosion rate reducing land degradation and ensuring environmental protection after the application of the appropriate soil conservation measures and planning tools.

## 2. Regional Setting

### Site Location

Atalanti watershed (Figure 1) is located at Fthiotida Prefecture in Central Greece (21°44'-24°39' longitudes and 37°45'-39°29' latitudes) with an area of approximately 248 km<sup>2</sup>, observing relatively gentle slopes in lowlands (almost 85% of the slopes are up to 20°) with flat relief and much steeper ones almost vertical cliffs in highlands where rocky formations prevail (>30° up to 2.5%). The river basin is surrounded by hilly and mountain ranges (Mt. Chlomo) washed by the sea at the East (Lappas 2018). The flat and hilly terrain covers 76% of the whole basin area mostly concerning the coastal areas while the rest 24% belongs to mountainous areas. In particular, the watershed's elevation ranges between sea level and 1073 m (a.s.l.) with mean elevation of 275.3 m (a.s.l.) and elevation 50% of 210 m. The combined effect of water erosion and weathering processes as well as the geological and tectonic features are the key factors forming the current geomorphological conditions. Also, the Atalanti river basin is characterized by dendritic to sub-dendritic drainage network discharging into the Aegean sea which is dense within the flat relief (semi-permeable formations) getting sparse in the mountainous areas due to the intensively active tectonics (extensive surface discontinuity, fractures etc.) forming steep slopes and deep river beds especially when passing through carbonate rocks (typical V-shape rejuvenated valleys as a result of the active faulting zones). In general, there are only intermittent streams, namely, Alargino, Karagkiozis and Ag. Ioannis which flow towards the sea only during winter and spring. Finally, the area represents a typical Mediterranean climate with Csa type (by Köppen classification) characterized by mild wet winters and hot as well as dry summers with a rotation period of a wet and dry season in October and April, respectively. The mean over-annual precipitation ranges between 650-750 mm with observed higher precipitation values in the mountains (up to 1300 mm) and significantly lower in the lowlands (<450 mm) while the air temperature ranges between 16.5-18.0 °C (Lappas 2018).

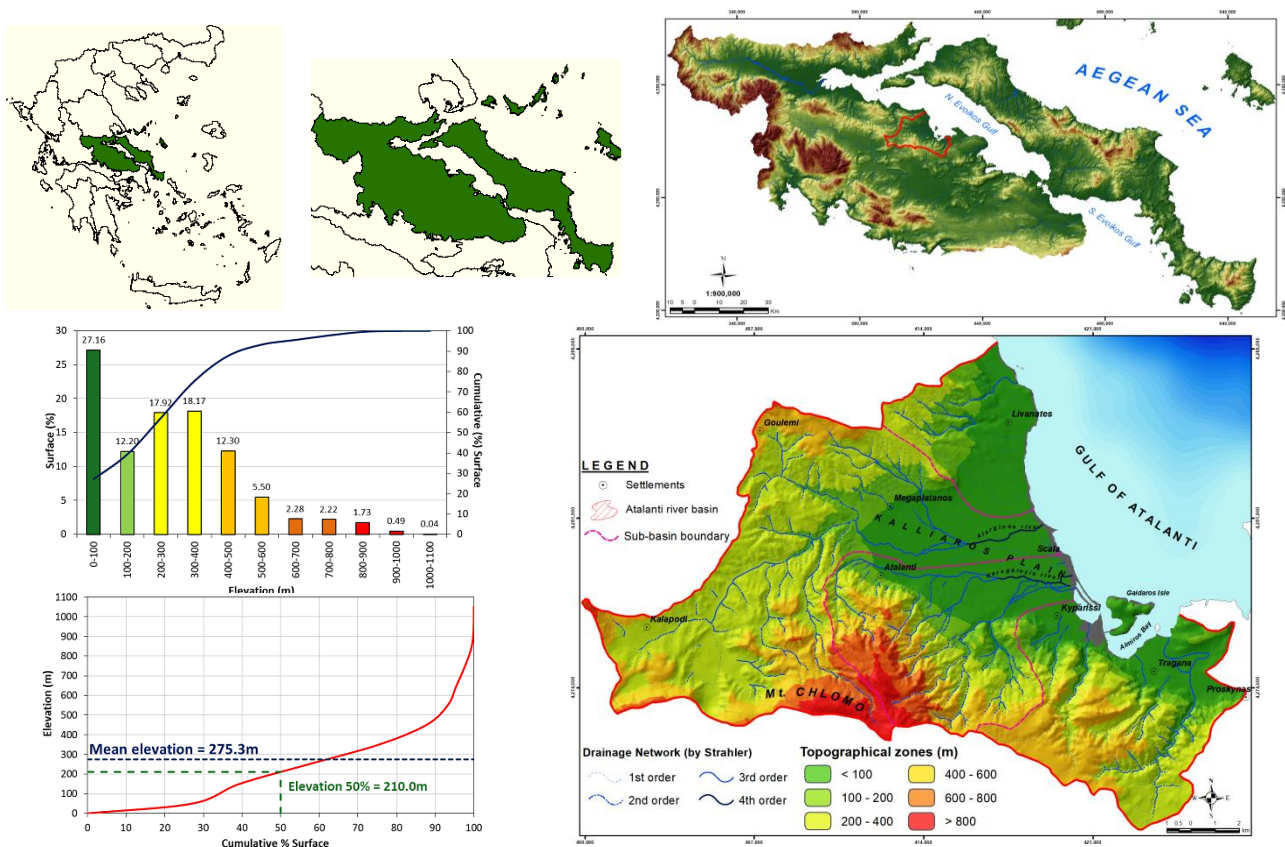


**Figure 1:** Site location of the study area, digital elevation model (DEM) of Eastern-Central Greece and topographical zones of Atalanti river basin with contributing drainage network and its hypsometric curve.

## 2.1 Geological Regime

As illustrated in Figure 2, the study area is consisted of several rocky formations including shales, sandstones, conglomerates (metamorphic-ultrabasic rocks of Paleozoic age), dolomites and limestones of different geological age (from Triassic to Cretaceous), ophiolitic rocks (diabases, peridotites, serpentines) and flysch as well. All the aforementioned geological formations comprise the bedrock along the eastern, northern and southern outcrops of the alluvial plain (Maratos et al. 1965). Moreover, post-alpine mostly unconsolidated sandy formations of Tertiary and Quaternary age consist of marls, marly limestones, sandy clay loams, sandy marls, conglomerates as well as lacustrine deposits such as clay-sandy sediments all derived from weathering of the surrounding mountain range alpine formations and mainly located at the lower parts of the basin in the coastal flat valley. Tectonically speaking, the most significant feature of the geological regime during Tertiary is the large-scale faulting zones with West-NorthWest and North-NorthEast directions reactivating many other faults also forming fractures, fissures, cracks and other discontinuities within the rocky beds. All these geological sediments and tectonic features along with the water's erosive and weathering capability may lead to faster erosion processes and consequently to the increase in soil detachment, transport and deposition towards the basins' lowlands with relatively high sediment discharge and yield along the river tributaries.

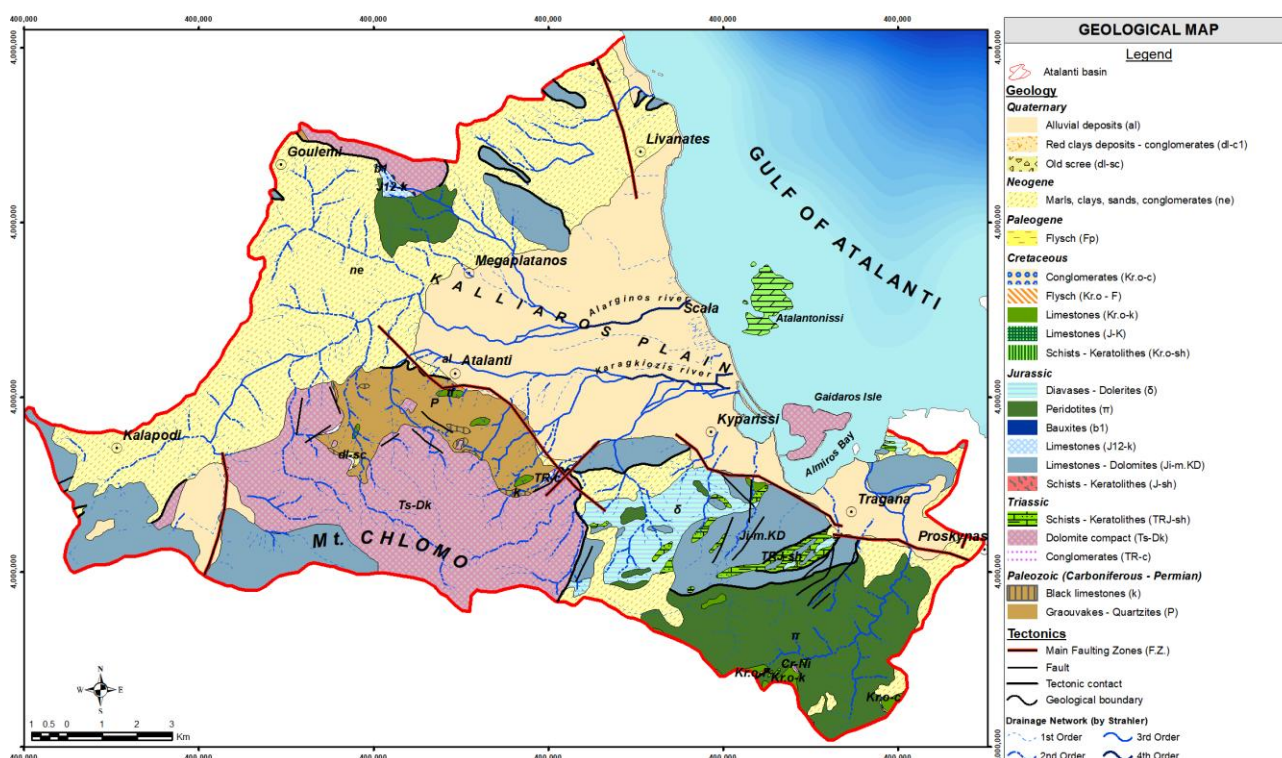


Figure 2: Geological map of Atalanti catchment (Maratos et al. 1965, with modifications by the authors).

### 3. Materials and Methods

#### 3.1 Input Data and Pre-Processing

In order to estimate the soil erosion (SE) and the sediment yield ( $S_y$ ) various data should be obtained and pre-processed. Firstly, topographical maps of 1:50,000 scales, obtained from the Hellenic Military Geographical Service (HMGS) are considered necessary to delineate the drainage network from which sediment load is transported to lowlands and contour maps (20m interval) with the aid of Digital Elevation Model (DEM of 25m grid cell resolution) of the watershed were used to calculate the slope gradient in degrees, the elevation difference, the flow accumulation and basin's physical characteristics as well. Moreover, adequate monthly hydrometeorological data such as temperature and precipitation were obtained (Hellenic National Meteorological Service-HNMS, Ministry of Environment and Energy) from various gauging stations within and nearby the study area for a significant time period (long timeseries) so as the temperature as well as the rainfall's spatial distribution and intensity to be derived as it is the main triggering factor for soil detachment. Also, through CORINE Land Cover Data (2012) the land use/land cover of the entire area was identified and categorized according to erodibility. Furthermore, soil type/texture map within the study area was extracted, produced and published by the Agriculture University of Athens to classify each soil for its erosivity. The required base maps of spatial data were pre-processed and analyzed in terms of watershed boundary, land use and rainfall maps as well as DEM and soil map in a Geographical Information System (GIS) environment to analyze and display spatial information so as to identify the areas within a given catchment that have similar erosion potential. Consequently, the final product would be a multi-layered map identifying areas of equal erosion potential.

#### 3.2 Methodology Analysis

Models developed to calculate soil erosion rate can be divided into empirical, conceptual and those based on physical processes. Empirical models such as the revised universal soil loss equation (RUSLE) (Renard et al. 1997, Wischmeier et al. 1978), as well as the Erosion Potential Model (EPM) (Gavrilovic 1988) are used worldwide to provide useful information to support soil and water conservation plans through a grid-based discretization map. Both the aforesaid models have been widely used to predict the average annual soil



loss, sediment yield and soil erosion rate in a raster GIS environment, however, they generally underestimate the total sediment yield since they cannot estimate and predict the gully erosion, the stream-channel erosion as well as the erosion caused by the wind.

### RUSLE

The RUSLE is an erosion model designed to predict the soil loss (Figure 3) caused by runoff in specified cropping and management systems. The RUSLE model computes the long term average annual soil loss/erosion ( $SE$  in  $tn/ha/yr$ ) expected on hillslopes by multiplying several factors in raster data format as follows (Renard *et al.*, 1997):

$$SE = R \times K \times (L \times S) \times C \times P \quad (1)$$

where:

$R$  is the rainfall-runoff erosivity factor ( $MJ \cdot mm/ha/h/yr$ ). The greater the intensity and duration of the rainfall, the higher the erosion potential.

$K$  is the soil erodibility factor ( $tn \cdot h/MJ/mm$ ) being a measure of the susceptibility of soil particles to detachment and transport by rainfall and runoff.

$L$  is the slope length factor (dimensionless). The longer the slope, the higher the risk for erosion.

$S$  is the steepness factor (dimensionless). The steeper the slope, the higher the risk for erosion.

$C$  is the cover management factor (dimensionless). It is used to determine the relative effectiveness of soil and crop management systems in terms of preventing soil loss and

$P$  is the erosion control-support practice factor such as cross-slope cultivation, farming direction, strip cropping, buffer strips, terraces etc. (dimensionless).

Each RUSLE factor was calculated in GIS interface and all factors were analyzed together in the model to predict the potential soil loss in a spatial domain within each cell-grid pixel at the study area (Bosco *et al.* 2015, Panagos *et al.* 2015a). The RUSLE represents how climate, soil profile, topography-relief, vegetation, land management practices and land use interact each other through sheet and interrill soil erosion caused by raindrop impact and overland flow. The advantage of the RUSLE model is that it has been widely used and tested for both agricultural and forest watersheds over many years (Renard *et al.*, 1997). In this study, sediment yield ( $S_y$  in  $tn/ha/yr$ ) was calculated using the Sediment Delivery Ratio (SDR-dimensionless) according to the following equation (Stefanidis *et al.* 2018):

$$S_y = SDR \times SE \quad (2)$$

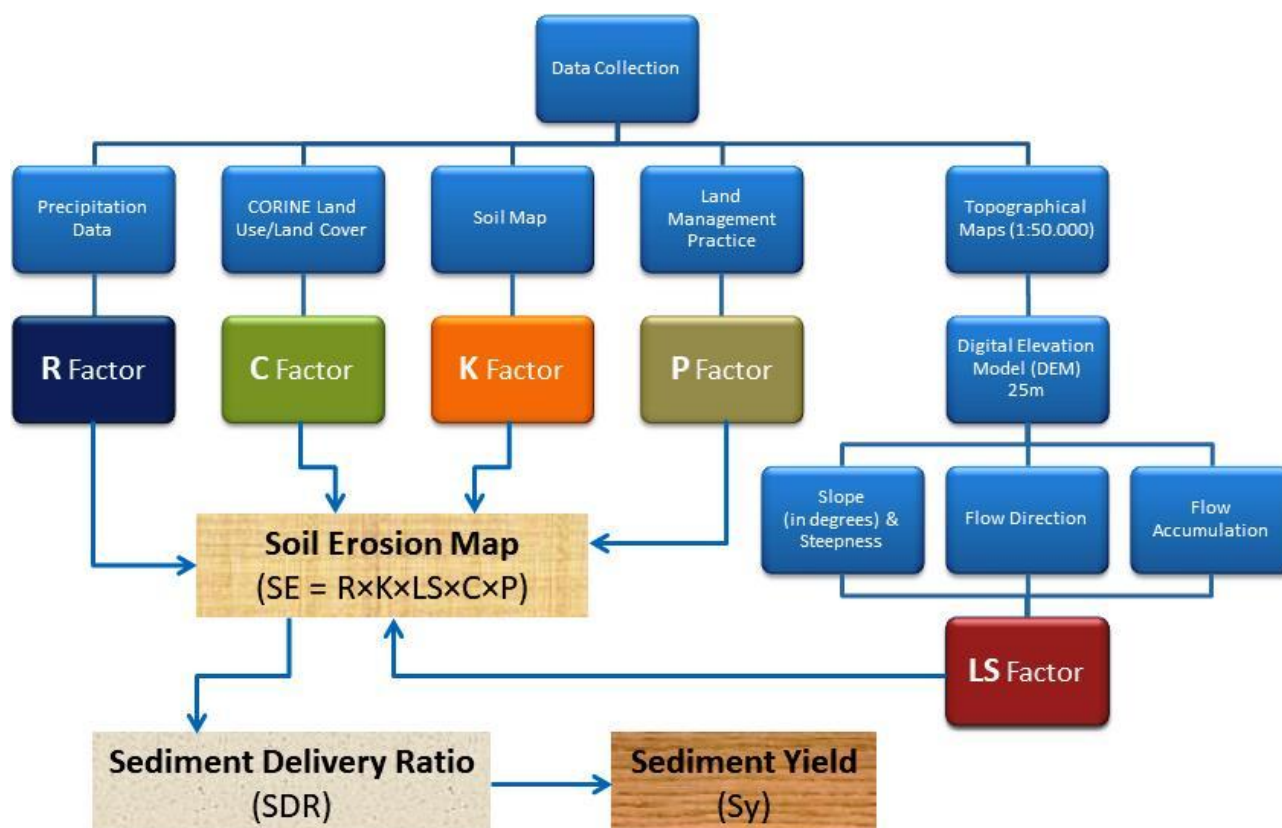


Figure 3: Flow chart of RUSLE methodology.

*EPM*The Erosion Potential Method (EPM-Gavrilocmethod) beingalso a widespread, empirical, semi-quantitative model(De Venteet al. 2005) used for qualifying the erosion severity and estimating the mean annual sediment yield and soil erosion rate on a catchment scale taking into account six individual factors, namely, geology, soil properties, topographic features, climate factors including mean annual rainfall and mean annual temperature, land use and degree of erosion (Figure 4). The most often calculated outputs of the method are the degree of annual soil loss (detached soil) $W_a$ , the erosion coefficient  $Z$  and the actual sediment yield  $S_y$  (eroded material transported through the river network). The average annual volume of detached soil ( $W_a$  in  $m^3/km^2/yr$ ) due to surface erosion is calculated as follows:

$$W_a = T \times R \times \pi \times Z^{3/2} \times F \quad (3)$$

where:

$T$  is the temperature coefficient (dimensionless)

$R$  is the mean annual amount of rainfall (mm)

$F$  is the basin's area ( $km^2$ ) and

$Z$  is the erosion coefficient (dimensionless).

The temperature coefficient  $T$  is calculated by the equation below:

$$T = [(T_o/10)+0.1]^{1/2} \quad (4)$$

where:

$T_o$  is the mean annual temperature ( $^{\circ}C$ ).

The coefficient of erosion  $Z$  is the measure of intensity of erosion processes given by the following equation:

$$Z = X \times Y \times (\varphi + J^{1/2}) \quad (5)$$

where:

$X$  is the soil protection coefficient (dimensionless)

$Y$  is the soil erodibility coefficient (dimensionless)

$\varphi$  is the type and extent of erosion coefficient (dimensionless) and

$J$  is the catchment's slope (%)

Only a fraction of the total sediment volume, produced within a catchment due to soil erosion results to the catchment's outlet since a large portion of that amount is deposited within, during the sediment's course towards the water bodies. Estimation of the effective sediment yield-specific annual sediment transport ( $S_y$  in  $m^3/km^2/yr$ ) in the outlet is made according to the parametric formula:

$$S_y = W_a \times SDR \quad (6)$$

where:

$SDR$  is the sediment delivery ratio (dimensionless) calculated as follows:

$$SDR = [(P \times H)^{1/2} / (L_p + 10)] \times D_d \quad (7)$$

where:

$P$  is the catchment's perimeter (km)

$H$  is the difference between the maximum catchment's elevation and catchment's outlet elevation (km) and

$L_p$  is the length of the principal waterway (km) and

$D_d$  is the drainage density ( $km/km^2$ ).

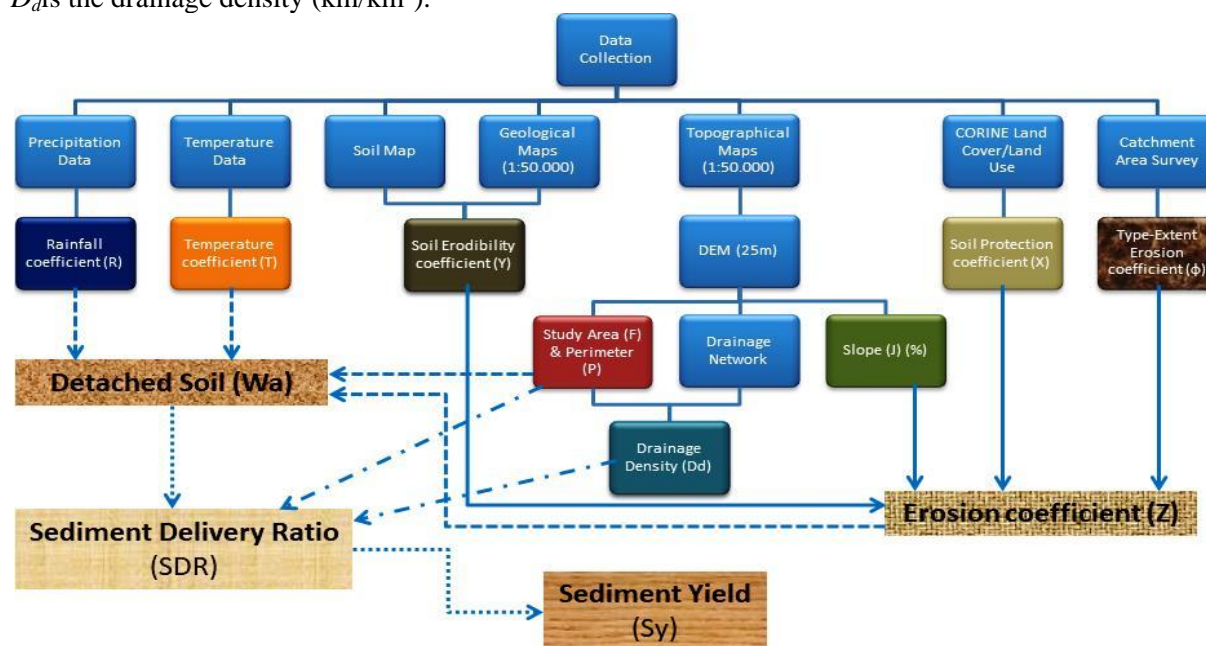


Figure 4: Flow chart of EPM-Gavrilovic methodology.

The EPM (Gavrilovic) method does not explore the physics of erosion processes and as such it is advantageous for areas where limited data are available or where there is a lack of previous erosion research. As such, the method provides an estimate not only of the amount of sediment production and sediment transport but also of the resulting erosion intensity indicating areas of potential erosion threats.

## 4. Results and Discussion

### 4.1 RUSLE Factors

#### Rainfall-Runoff Erosivity (R)

The R factor is an indication of the two most important characteristics of a storm determining its erosivity against the amount of rainfall and peak intensity, also having strong correlation with soil erosion. The R value is greatly affected by the volume, intensity, duration and pattern of rainfall and by the amount and rate of the resulting runoff. Mostly monthly and annual mean values of rain are used for R factor estimation in RUSLE model (Angulo-Martinez et al. 2012, Panagos et al. 2015b, 2017, Renard et al. 1994). In the present study, monthly rainfall data (Figure 5) of 43 years (1970-2012) from 17 adjacent rain gauge stations collected from the Hellenic National Meteorological Service (HNMS) and the Ministry of Environment and Energy were used to calculate R-factor (mean value) using the following most suitable for the regional area

equations.

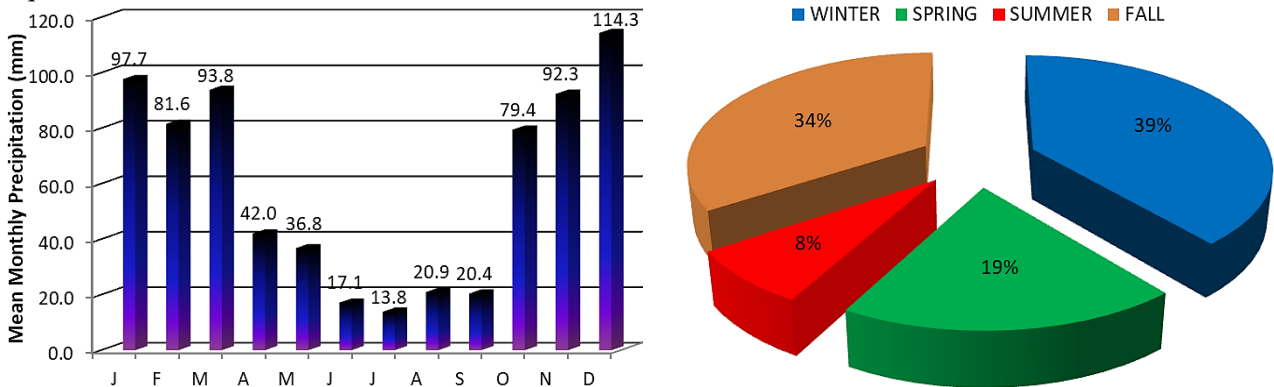


Figure 5: Mean monthly rainfall (left) and mean temporal distribution (right).

The R factor for each of the relationships below was estimated and the mean value of the resulted R factor was finally taken into consideration (Arnoldus 1980, Flambouris 2008, Kouli et al. 2008, Renard et al. 1991, Sigalos et al. 2010, Vahaviolos 2014, Van der Knijff et al. 2000, Wischmeier et al. 1978, Zarris et al. 2011):

$$R_1 = 0.612 \times MFI^{1.56} \text{ (Sicily-Italia)} \quad (8)$$

$$R_2 = 0.264 \times MFI^{1.50} \text{ (Morocco)} \quad (9)$$

$$R_3 = 1.3 \times P \quad (10)$$

where:  $P_i$  is the mean monthly rainfall (mm)

$P$  is the mean over-annual rainfall (mm) and

$MFI$  is the modified Fournier index (dimensionless) given by the equation:

$$MFI = (P_1 + P_2 + \dots + P_{12}) / P \quad (11)$$

The spatial interpolation techniques in a GIS environment were used for estimating the spatial variability both for rainfall and rainfall-runoff erosivity factor (R) in the study area (Figure 6). The larger numbers of R factor the more erosive conditions.

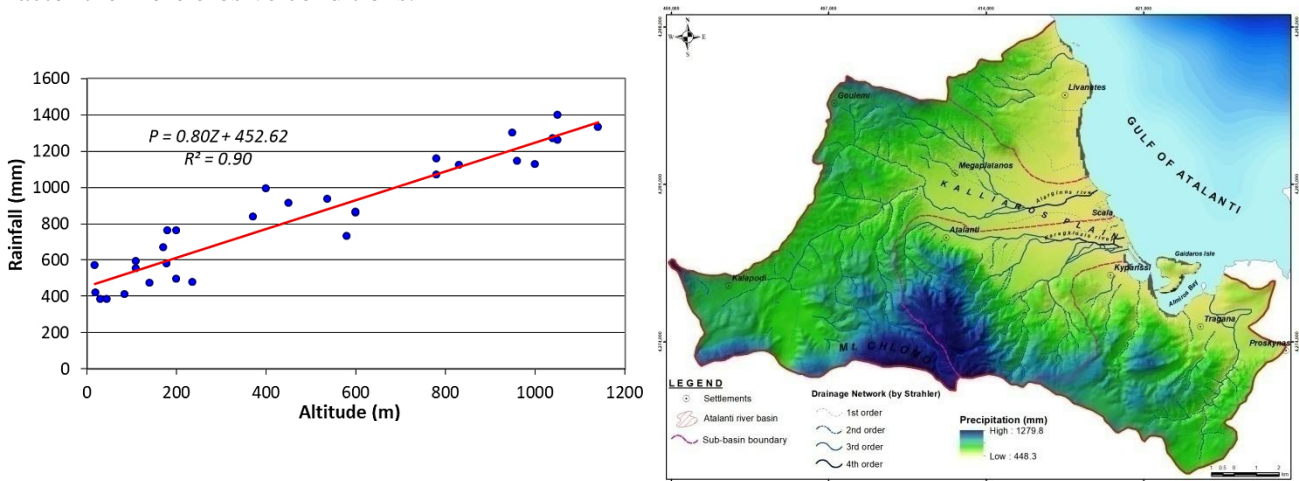


Figure 6: Rain gradient equation according to linear regression analysis (left) and precipitation spatial distribution in Atalanti river basin (right).

The mean values of the R factor range from 350 MJ-mm/ha/h/yr for the Ag. Ioannis sub-watershed to 1212.1 MJ-mm/ha/h/yr for both Alarginos and Karagkioziss sub-watersheds. The calculated R factors were subdivided into classes showing high erosivity in the regional area of Chlomo Mountain and medium to lower erosivity in the central and eastern part of Atalanti river basin. As the topography changes going from steep (mountainous areas) to flat relief (coastal areas) the erosivity gradually decreases reaching 348 MJ-mm/ha/h/yr (Figure 7).

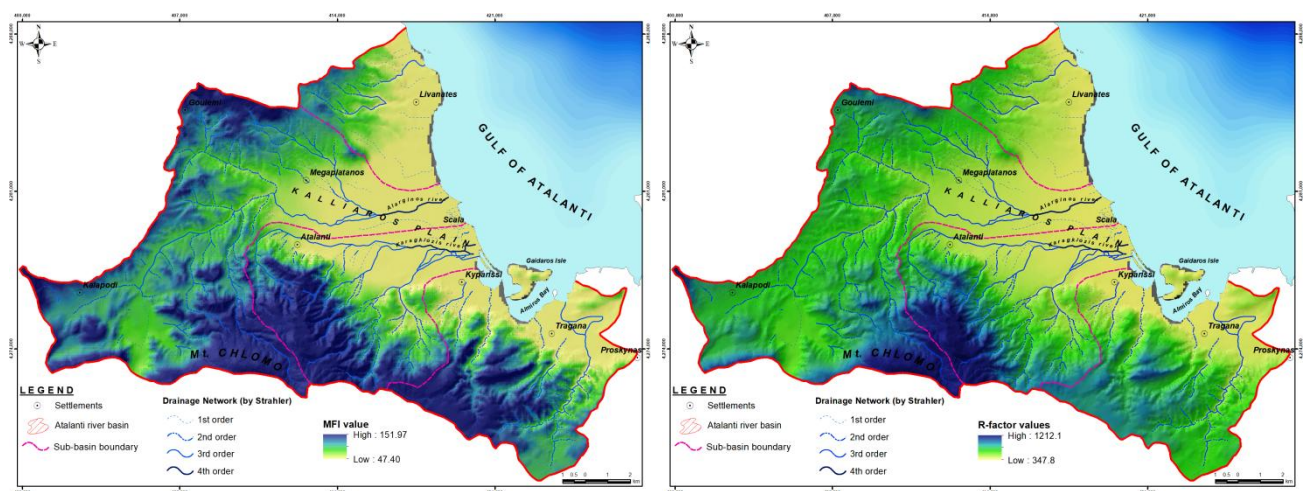


Figure 7: MFI value and R factor spatial distribution.

Soil Erodibility (K)

The K factor represents the susceptibility of soil or surface material to erosion. A generalized soil texture map collected from the Agricultural University of Athens (Yasoglou 2004) in scale 1:850.000, combined with the geological maps produced by the Institute of Geology and Mineral Exploration (IGME) in scale 1:50.000 and literature reviews was used for the estimation of K factor map (Table 1, Figure 8) on the basis of soil textures. In fact, finer textured soils, rich in clay, are more resistant to particles detachment while coarser textured soils allow to a high infiltration of water, avoiding superficial runoff. The soil types were grouped into eight (8) main classes with varying soil characteristics while the corresponding K values for the soil types were identified from the soil erodibility nomograph by considering the particle size, organic matter content and permeability class. The K factor is a numerical value which ranges from 0 to 1 with soil erodibility values closer to 1 being most prone to soil erosion. The highest values of the soil erodibility factor are spatially well correlated with the areas which expose Quaternary and Neogene sediments (Alewell et al. 2015, Kouli et al. 2008, Lappas 2018, Montgomery 2007, Oikonomidis et al 2014, Sigalos et al. 2010).

Table 1: K-factor values.

Geological Formation	Soil Erodibility Factor (K)	Area (km <sup>2</sup> )	Area (%)
Ophiolites/Bauxites	0.0005	32.5	13.12
Limestones/Dolomites	0.0007	70.3	28.38
Conglomerates	0.003	0.2	0.08
Alluvial deposits	0.0035	58.5	23.62
Debris	0.045	0.1	0.04
Marls, Clays	0.005	72.4	29.24
Flysch/Schist	0.025	2.0	0.81
Graouvakes/Tuffs	0.015	11.7	4.71

Slope Length and Steepness (LS)

The LS factor represents the effect of slope length (L) and steepness (S) on erosion which are simultaneously computed in form of a LS factor. The soil loss per unit area increases as both the slope length and steepness increase as high slope accelerates the velocity of surface runoff also increasing the amount of cumulative runoff, hence, the soil erosion rate (McCool et al. 1987). The combined LS factor was computed for the watershed by means of GIS environment, via DEM, given by the following equation (Mitasova et al. 2001, Panagos et al. 2015d):

$$LS = [(A_s/22.13)^m] \times [(sin\beta \times 0.01745/0.0896)^n] \quad (12)$$

$$LS = [(FlowAccumulation \times resolution/22.13)^{0.4}] \times [(sinSLOPE_{(deg)} \times 0.01745/0.0896)^{1.4}] \quad (13)$$

where:  $A_s$  is the flow accumulation (the accumulated upslope contributing area for a given cell size,  $25 \times 25$  m) and  $\beta$  is the mean basin's slope (in degrees).

The highest values of the coefficient are met at high relief areas while the lowest at the catchment lowlands gradually declining towards its outlet (Figure 8). The LS factor value in the study area varies from 0 to 22.47 with mean and standard deviation of 3.67 and 6.65, respectively.

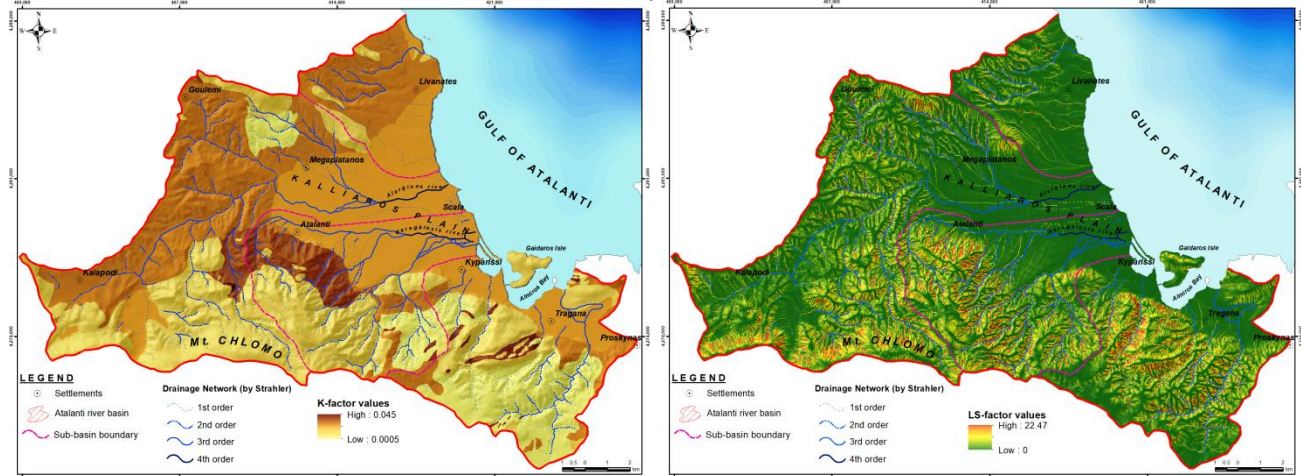


**Figure 8:** K and LS factors' spatial distribution.

Vegetation Cover Management (C)

The C factor represents the effect of cropping and management practices on soil erosion vulnerability rate in agricultural lands as well as the degree of protection from erosion provided by crops, vegetation etc. The temporal differentiation of C-factor is based on many factors like rainfall, agricultural practice, type of crops etc. The C factor varies from near zero for a well-protected land cover (high vegetation cover) to 1 for bare soil areas with mild or low vegetation cover, thus, the impact of C factor on soil erosion is less important when the land use/land cover comprises high percent of forest and plantation crops. In this study case the cover management factor C (Table 2, Figure 9) was prepared on the basis of CORINE land cover/land use map assigning seven (7) classes which range between 0.001 and 0.3. This equation was successfully applied for assessing the C-factor of areas with similar terrain and climatic conditions (Alkharabsheh et al. 2013, Lappas 2018, Efthimiou et al. 2014, 2016a, 2016b, Panagos et al. 2015c, Pham et al. 2018, Wischmeier et al. 1978).

**Table 2:** C-factor values.

CORINE Land Cover/Land Use	Cover Management Factor (C)	Area (km <sup>2</sup> )	Area (%)
Vineyards	0.2	0.3	0.12
Olive groves/Land with natural vegetation	0.1	58.5	23.61
Complex cultivation patterns	0.18	29.3	11.82
Broad-leaved/Coniferous/Mixed forest	0.001	8.7	3.51
Natural grasslands/Non-irrigated arable land	0.3	54.4	21.95
Sclerophyllous vegetation	0.03	72.4	29.22
Transitional woodland-shrub	0.02	24.2	9.77

Conservation-Support Practice (P)

The P factor (Table 3, Figure 9) is the soil loss ratio with a specific support practice ranging from 0 to 1 in which the highest value is assigned to areas with no conservation practices (open areas, grasslands

etc.) whereas the minimum values correspond to built-up-land indicating good conservation practice (Panagos et al. 2015e, Silva et al. 2014, Vahaviolos 2014, Xanthakis et al. 2017).

**Table 3:** P-factor values.

CORINE Land Cover/Land Use	Support Practice Factor (P)	Area (km <sup>2</sup> )	Area (%)
Vineyards/Complex cultivation patterns	0.75	29.6	11.95
Non-irrigated arable land	0.80	26.4	10.65
Olive groves/Land with natural vegetation	0.85	58.5	23.61
Broad-leaved/Coniferous/Urban fabric/Mixed forest/Natural grasslands/Sclerophyllous vegetation/Transitional woodland-shrub	1.00	133.3	53.79

Soil Loss/Erosion (SE)

After applying the equation (1) in Alarginos sub-basin the mean over-annual Soil Loss/Erosion rate ranges from 0 to 516.1 tn/ha/yr with mean value and standard deviation of 5.02 and 19.87, respectively, in Karagkiozis sub-basin the mean over-annual Soil Loss/Erosion rate ranges from 0 to 459.8 tn/ha/yr with mean value and standard deviation of 4.21 and 16.32, respectively and in Ag. Ioannis sub-basin the mean over-annual Soil Loss/Erosion rate ranges from 0 to 118.2 tn/ha/yr with mean value and standard deviation of 2.19 and 17.11, respectively (Figure 10).

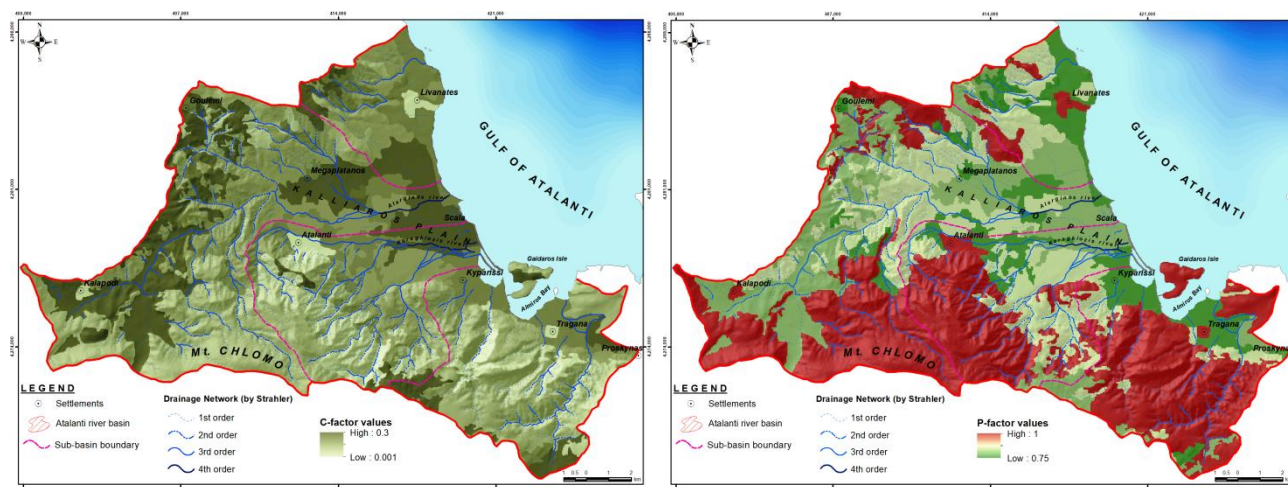


**Figure 9:** C and P factors' spatial distribution.

Sediment Delivery Ratio (SDR)

Sediment delivery ratio is a coefficient which gives the amount of eroded materials in a watershed that are transported to the basin's outlet. In order to estimate this ratio empirical methods and relations are used, several of which are given by the following equations:

$$SDR_1 = 0.42 \times A^{-0.125} \text{ Vanoni (1975)} \tag{14}$$

$$SDR_2 = 0.51 \times A^{-0.11} \text{ USDA SCS (1971)} \tag{15}$$

$$\log(SDR_{3-1}) = 1.7935 - 0.14191 \times \log(A) \text{ (Renfro 1975)} \tag{16}$$

$$\log(SDR_{3-2}) = 2.9426 + 0.82362 \times \log(R/L) \text{ (Renfro 1975)} \tag{17}$$

where:

$A$  is the catchment area (in  $\text{km}^2$  according to Renfro equation and in  $\text{mi}^2$  according to Vanoni and USDA equations)

$R$  is the difference between the maximum and minimum (outlet) basin's elevation (m) and

$L$  is the longest waterway for each basin (km).

The final SDR value was calculated taking into account the mean value derived from all the above equations.

Sediment Yield ( $S_y$ )

After applying the equation (2) the mean Sediment Yield ( $S_y$ ) for each sub-basin, namely, Alarginos, Karagkiozis and Ag. Ioannis, equals to 2.63, 1.82 and 0.61  $\text{tn/ha/yr}$ , respectively (Table 4, Figure 10).

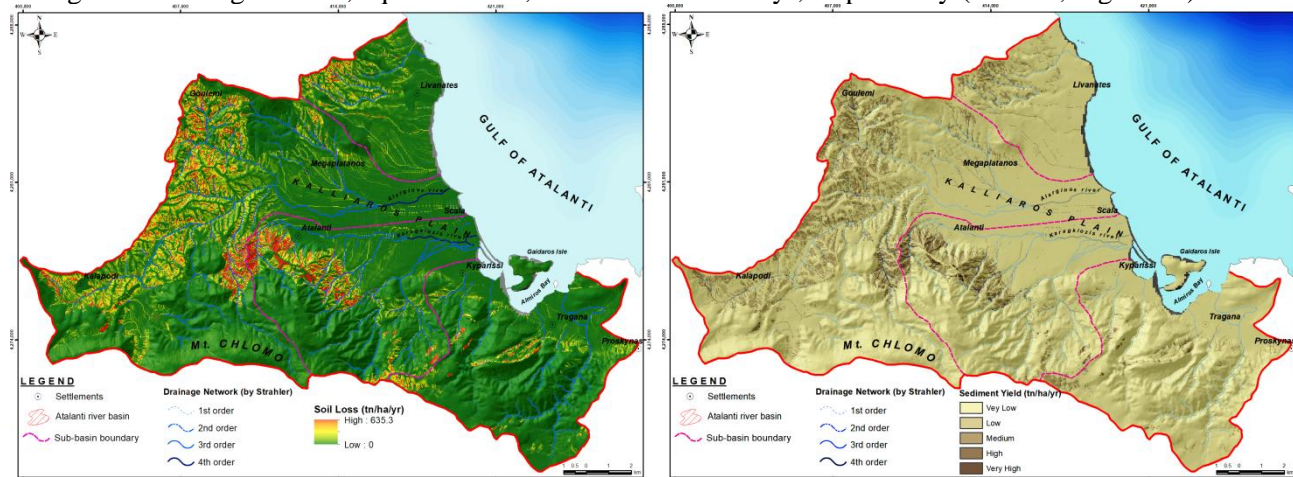


**Figure 10:** Soil Loss/Erosion (SE) (left) and Sediment Yield ( $S_y$ ) (right) spatial distribution in Atalanti river basin.

**Table 4:** Mean annual Sediment Yield ( $S_y$ ) calculation for each sub-basin based on RUSLE method.

Sub-basin	Area ( $\text{km}^2$ )	Soil Loss/Erosion (SE) ( $\text{tn/ha/yr}$ )	Sediment Delivery Ratio (SDR)	Sediment Yield ( $S_y$ ) ( $\text{tn/ha/yr}$ )
Alarginos	109.05	8.78	0.299	2.63
Karagkiozis	55.18	5.56	0.327	1.82
Ag. Ioannis	46.26	1.83	0.334	0.61

As illustrated in Figure 10 (right), the max  $S_y$  derives from the mountainous areas where steep and abrupt slopes prevail while in the flat relief neither soil loss nor sediment yield take place

**4.2EPM Coefficients**

This method considers six factors depending on surface geology and soils, topographic features, climatic factors (including mean annual rainfall and mean annual temperature) and land use as well. The temperature coefficient (T) is estimated concerning the basin's normalized mean annual temperature taking into account all the available meteorological stations of the regional area, that is, ten-10 stations around the study area. The mean annual temperature (Figure 11) equals to  $16.7^{\circ}\text{C}$  with the max temperature values taking place during the summer (dry period) and the min ones during the winter (wet period) (typical Mediterranean climate). The regression analysis (temperature gradient) gives the opportunity to spatially distribute the temperature showing the cold and warm areas within the catchment.

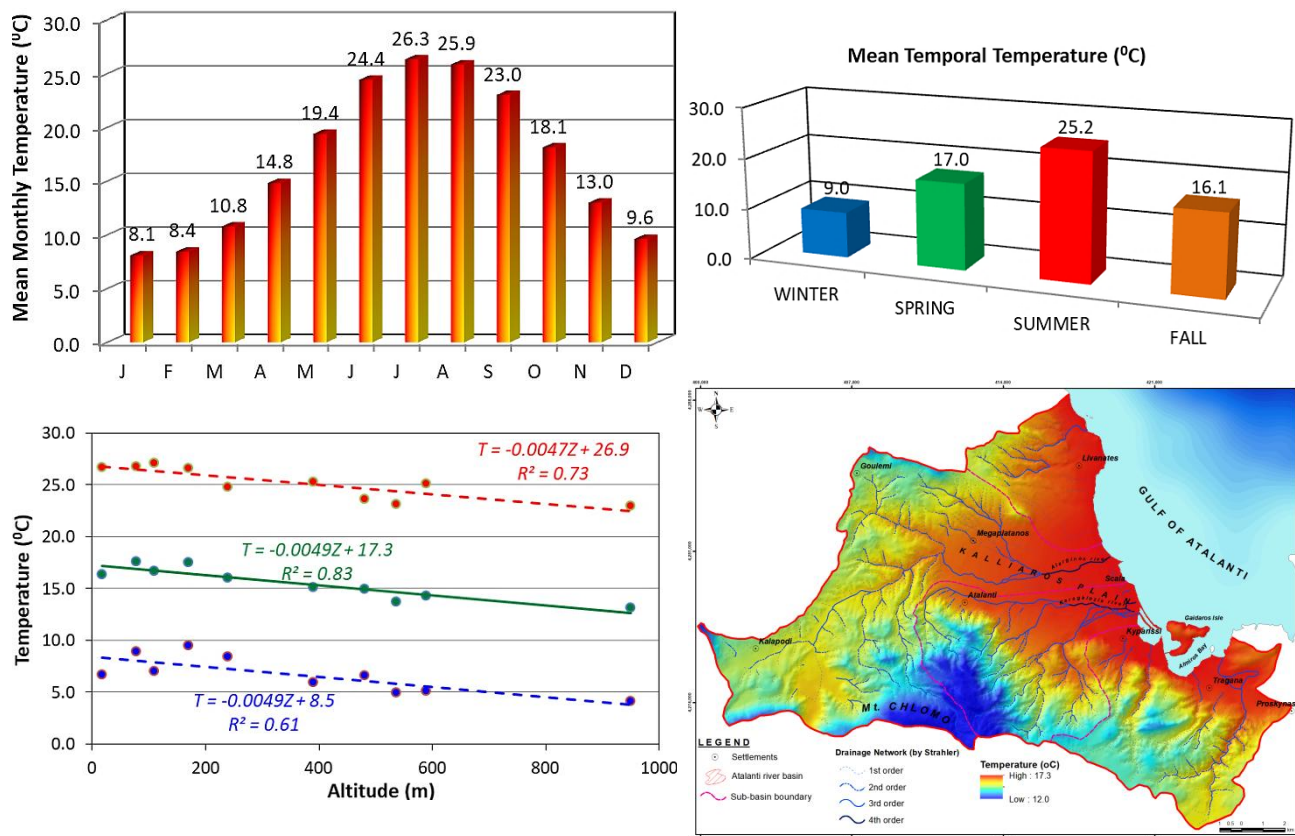


**Figure 11:** Mean monthly temperature (up left), mean temporal distribution (up right), min (blue dashed line) – max (red dashed line) – avg (green solid line) temperature gradient equation according to linear regression analysis (down left) and temperature spatial distribution in Atalanti river basin (down right).

Soil Protection (X)

It depends on land use, vegetation cover and the measures taken to reduce erosion agriculture activities expressed as the protection of an area against precipitation and erosion. Its values range from 0.05 (e.g. high density forest land) to 1.0 (e.g. areas without vegetation cover). Taking into consideration the CORINE Land Cover 2000 classification every land use was assigned to a value (Table 5) estimated by the use of EPM guide table (Gavrilovic 1988, Brambilla et al. 2011, Dragicevic 2016, Dragicevic et al. 2017). The lowest values occur at areas of high vegetation cover denoting the protective effect of the latter against soil erosion, whilst the highest at areas of mild or low vegetation cover (Figure 12).

**Table 5:** X-coefficient values.

CORINE Land Cover/Land Use	Soil Protection Coefficient (X)	Area (km <sup>2</sup> )	Area (%)
Vineyards/Olive groves/Land with natural vegetation	0.8	58.8	23.73
Broad-leaved/Coniferous/Mixed forest	0.05	8.7	3.51
Natural grasslands/Transitional woodland-shrub	0.6	27.5	11.10
Non-irrigated arable land	0.9	51.1	20.62
Sclerophyllous vegetation	0.4	72.4	29.22
Complex cultivation patterns	0.7	29.3	11.82

Soil Erodibility (Y)

It depends on geology and soil texture expressed as the inverse value of the soil resistance to erosion due to the precipitation's erosive force. Its values range from 0.2 (hard rock) to 2.0 (coarse sediments). According to the geological map (Figure 2), a Y coefficient value was assigned to every coded geological formation met in each catchment (Gavrilovic 1988, Dragicevic et al. 2017), that being, the hard rocks which are resistant to erosion processes are the ophiolites and bauxites while the geological formations prone most to erosion are the conglomerates, the marls and the debris (Table 6, Figure 12). Overall, eight (8) lithological formations were classified based on their erosion sensitivity.

**Table 6:** Y-coefficient values.

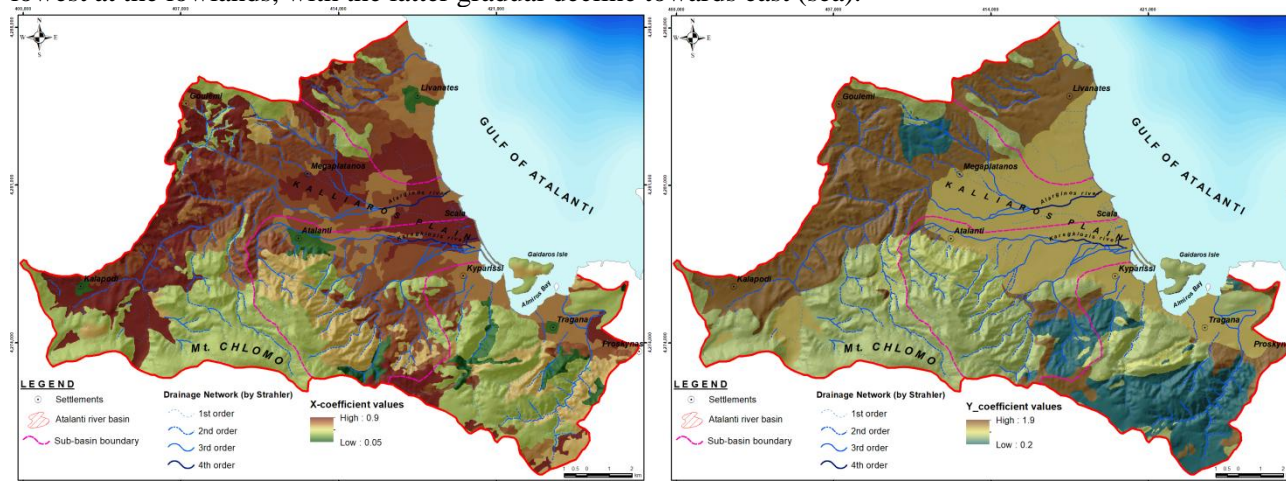
Geological Formation	Soil Erodibility Coefficient (Y)	Area (km <sup>2</sup> )	Area (%)
Ophiolites/Bauxites	0.2	32.5	13.12
Limestones/Dolomites	0.8	70.3	28.38
Conglomerates	1.6	0.2	0.08
Alluvial deposits	1.3	58.5	23.62
Debris	1.9	0.1	0.04
Marls, Clays	1.7	72.4	29.24
Flysch/Schist	1.0	2.0	0.81
Graouvakes/Tuffs	0.9	11.7	4.71

Type and Extent of Erosion (φ)

The φ coefficient values were determined after field observation surveys carried out to identify the erosion processes ranging between 0.1 (limited erosion) to 1.0 (watershed affected by erosion) (Gavrilovic 1988). The Atalanti river basin is regarded as a limited erosion area, thus ranging between 0.1 and 0.2 (Figure 12).

Catchment's slope (J)

The area's slope (%) was calculated based on the DEM (25m grid cell resolution) through GIS implementation after digitizing 1:50.000 topographical maps. The slopes were re-classified into seven (7) categories ranging from 0–5 to >45% (Figure 12). The highest values occur at high relief areas while the lowest at the lowlands, with the latter gradual decline towards east (sea).



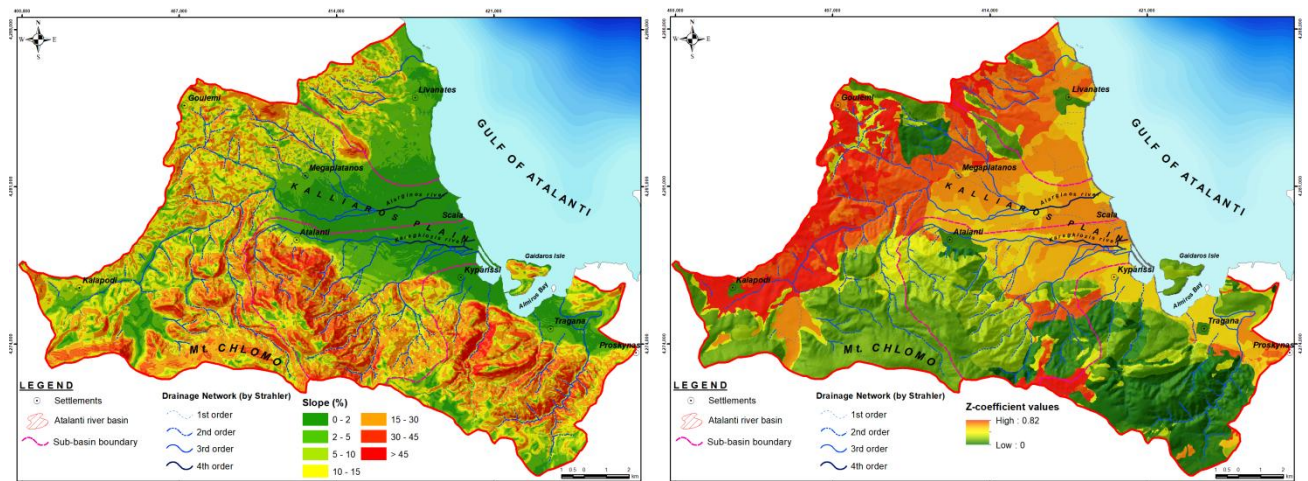


Figure 12: X, Y, J and Z coefficients' spatial distribution.

Considering the spatial distribution of all the above input data the model was implemented in a GIS-based environment, leading to the estimation initially of the erosion severity coefficient Z (Figure 12) and afterwards the detached soil volume ( $W_a$ ) as illustrated in Figure 13. There seems that slope does not affect the final result as much.

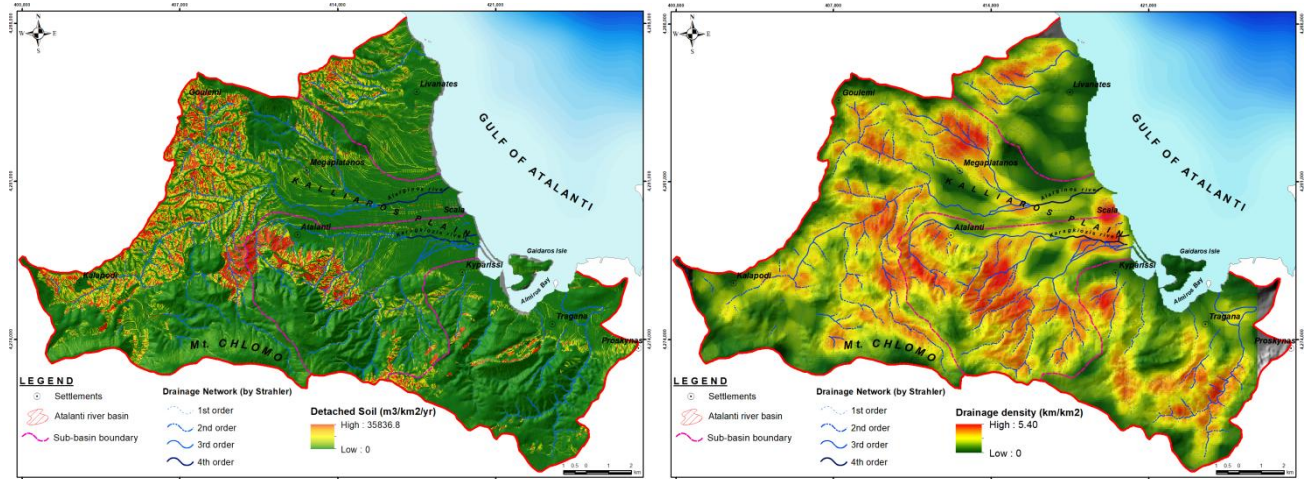


Figure 13: Detached soil volume ( $W_a$ ) estimation (left) and Drainage density ( $D_d$ ) distribution (right).

After estimating the Z-coefficient and detached soil volume ( $W_a$ ), it is necessary to determine the proportion of sediments that reach to the rivers since only a fraction of the total sediment volume results to the basin's outlet (transported material). A large portion of the produced sediment is deposited towards the streams. Therefore, sediment delivery ratio (SDR) has to be determined first so the sediment yield to be estimated afterwards (Table 7).

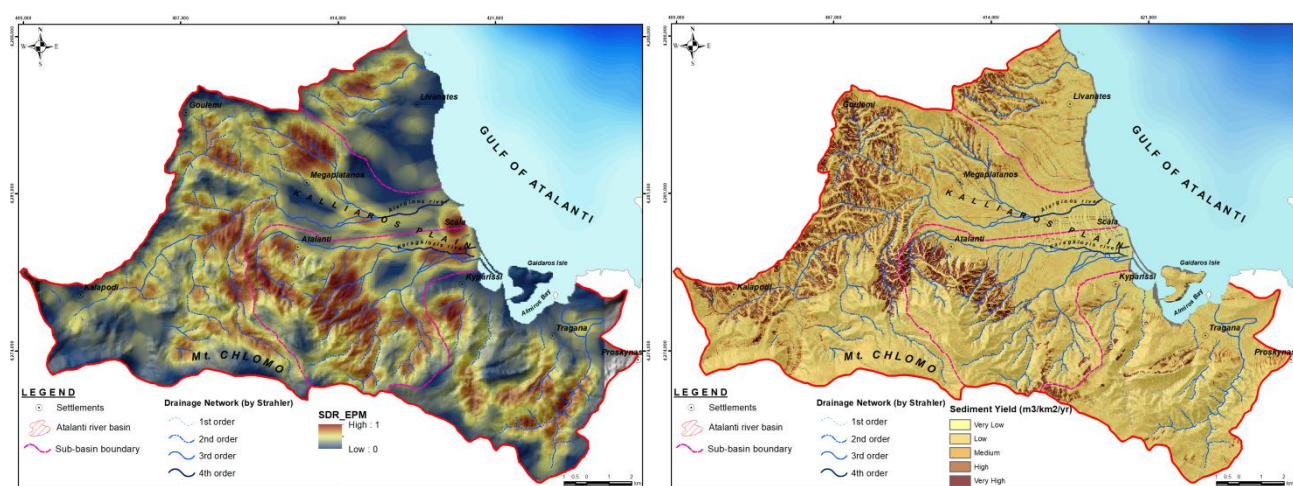


Figure 14: Sediment Delivery Ratio (SDR) (left) and Specific Yield ( $S_y$ ) estimation (right).

Table 7: Mean annual Sediment Yield ( $S_y$ ) calculation for each sub-basin based on EPM method.

Sub-basin	Area (km <sup>2</sup> )	Detached Soil ( $W_a$ ) (m <sup>3</sup> /km <sup>2</sup> /yr)	Sediment Delivery Ratio (SDR)	Sediment Yield ( $S_y$ ) (m <sup>3</sup> /km <sup>2</sup> /yr)
Alarginos	109.05	348.53	0.367	127.91
Karagkiozis	55.18	223.86	0.394	88.20
Ag. Ioannis	46.26	90.34	0.408	36.86

As illustrated in Figure 14 (right), the max  $S_y$  derives from the highlands while in lowlands no sediment yield takes place whatsoever.

### 4.3 Erosion Estimation Results

Both models were implemented annually making more or less the same assumptions so as the results to be comparable. Thus, comparing RUSLE and EPM methods one can observe that the EPM values of mean annual sediment yield for the main sub-basins were slightly higher than those estimated by RUSLE (Table 8).

Table 8: Mean annual Sediment Yield ( $S_y$ ) comparison for each sub-basin based on RUSLE and EPM methods.

Sub-basin	Area (km <sup>2</sup> )	RUSLE		EPM	
		Sediment Yield ( $S_y$ ) (tn/ha/yr)	Sediment Yield ( $S_y$ ) (m <sup>3</sup> /km <sup>2</sup> /yr)	Sediment Yield ( $S_y$ ) (tn/ha/yr)	Sediment Yield ( $S_y$ ) (m <sup>3</sup> /km <sup>2</sup> /yr)
Alarginos	109.05	2.63	110.46	3.05	127.91
Karagkiozis	55.18	1.82	76.44	2.11	88.20
Ag. Ioannis	46.26	0.61	25.62	0.88	36.86

The different results are initially attributed to the degree of reliability of the factors and coefficient estimated since there is lack of measurable data such as actual sediment discharge measurements. Moreover, the soil erosion mechanism is by itself a complex procedure so by multiplying many coefficients and factors together makes the final results even more ambiguous. Also, the catchment's soil properties were described through its lithology while organic matter content is absent and therefore discarded. Furthermore, the vegetation cover may alter within a year so only estimations can be made. It is pointed out that the models perform better in highlands than in lowlands due to abrupt relatively changing properties such as the precipitation erosivity, geology-topography-land cover pattern combinations allowing high erosion rates as well as significant sediment discharge values.

**Table 9:** RUSLE and EPM sediment yield classes.

Sediment Yield (S <sub>v</sub> ) classes	RUSLE		EPM	
	Area (km <sup>2</sup> )	Area (%)	Area (km <sup>2</sup> )	Area (%)
Very Low	93.49	37.73	81.29	32.81
Low	105.02	42.38	92.82	37.45
Medium	41.43	16.72	60.91	24.58
High	6.24	2.52	9.34	3.77
Very High	1.62	0.65	3.44	1.39

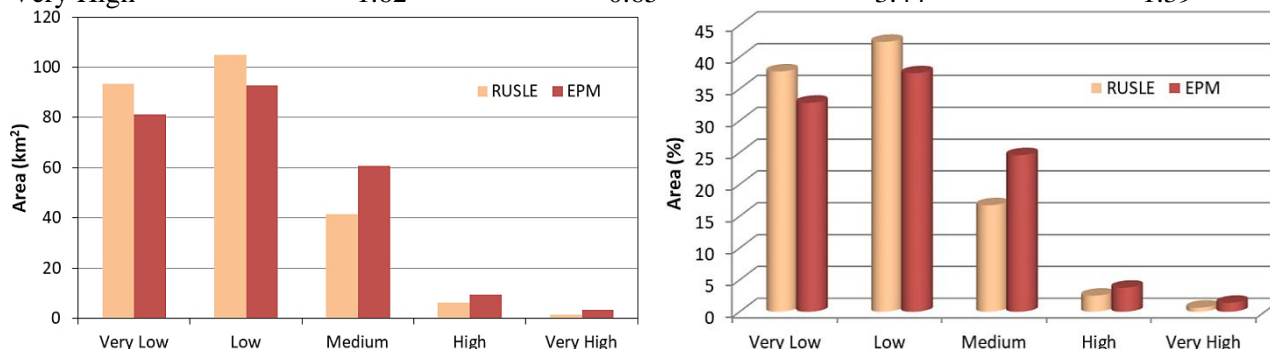


**Figure 15:** Bar and pie charts showing the area occupied by the different sediment yield classes based on RUSLE and EPM methods.

Based on the extent of erosion area (Table 9, Figure 15) in Atalanti watershed showed that approximately 80% and 69% for RUSLE and EPM methods, respectively, of the total areas occupied by Very Low and Low classes scattered in all over the study area while only 3% and 5.2% respectively belong to High and Very High classes. The Low-Very Low classes represented the lowlands (flat to gentle slopes) where the low slope gradient allows the accumulation of materials transported by water or gravity. On the other hand, the increasing of soil loss amount is mainly due to greater inclinations in comparison with the previous landforms. The most dangerous situation (High-Very High classes) was found in accordance to abrupt and steep slopes as well as low vegetation cover. This is because the vegetation of ground cover plays an important role in protecting surface soil from direct impact of rain water. Finally, these two models allowed identification of the most susceptible areas to water erosion also providing an adequate basis in terms of a preliminary approximation.

## 5. Conclusions

The present study was conducted in the Atalanti catchment, located in central-eastern Greece to assess the applicability of the empirical soil erosion models of RUSLE and EPM integrated with GIS techniques for basin's soil erosion potential, sediment production, detached soil and actual sediment yield estimation. Using GIS techniques, it was possible to identify and map the areas most susceptible to erosion as well as to analyze the soil loss rates even if the available data are limited. Since no field data have been ever collected in the study area, no calibration neither verification nor validation of the models' performance could be taken into account. Factors as land cover, erosion degree, soil texture and erodibility factors, topography, climate conditions and geology are important to control the runoff and consequently, the erosion process. Although such methods easily and rapidly model areas with erosion severity, it has to be noticed that the accuracy of analyzed data primarily depends on the expert judgement who determines the values of erosion coefficients. After implementation of these methods, both performed quite similarly, with the EPM model to obtain slightly higher values of sediment yield. Under the examined conditions, low erosion rates and sediment yield were due to the low to intermediate erosive capacity of the rainfall factor and occur in areas of gentle slopes and vegetation providing adequate soil protection. Intermediate values occur in areas of steeper slopes and vegetative cover such as dense native forest and rangelands which provides some protection while high erosion rates occur on steep slopes (>30%), degraded vegetative cover (e.g. sparse native forest) and on fallow/abandoned/bare lands. Erosion mapping through both methods showed to be



useful tools for environmental monitoring and water resources management which could provide satisfactory results when jointly used and the estimated sediment yield showed significant value variability ranging from very low to very high class. The predicted amount of soil loss and its spatial distribution can provide a basis for special priority to affected areas from high and severe soil erosion for the implementation of control measures with respect to soil conservation practices and land preservation from degradation. In conclusion, the two models performed quite sufficiently allowing map identification and visualization of the most prone to erosion areas.

### Acknowledgements

The authors would like to express their thanks to the Hellenic Military Geographical Service (HMGS) for the topographical maps, scale 1:50.000, obtained as well as the Hellenic National Meteorological Service (HNMS) and the Ministry of Environment and Energy for the hydrometeorological stations' precipitation and temperature dataset of the regional area.

### Conflict of Interests

The authors confirm that there is no conflict of interests referred to in the paper.

### References

- Alkharabsheh M., Alexandridis T., Bilas G., Misopolinos N., Silleos N. (2013). Impact of land cover change on soil erosion hazard in northern Jordan using remote sensing and GIS. *Procedia Environmental Sciences*, pp.912-921.
- Angulo-Martínez M., Beguería S. (2012). Trends in rainfall erosivity in NE Spain at annual, seasonal and daily scales, 1955–2006. *Hydrol. Earth Syst. Sci.*, pp.3551-3559.
- Arnoldus J. (1980). An approximation of the rainfall factor in the Universal Soil Loss Equation, in: *Assessment of Erosion*, edited by: De Boodt, M., Gabriels, D., Chichester, New York, pp.127-132.
- Bosco C., De Rigo D., Dewitte O., Poesen J., Panagos P. (2015). Modelling soil erosion at European scale: towards harmonization and reproducibility. *Natural Hazards and Earth System Sciences*, pp.225-241.
- Brambilla D., Longoni L., Mazza F., Papini M. (2011). Sediment yield from mountain slopes: a GIS based automation of the classic Gavrilovic method. *Transactions on Ecology and the Environment*, pp.301-311.
- De Vente J., Poesen J. (2005). Predicting soil erosion and sediment yield at the basin scale: scale issues and semi-quantitative models. *Earth Sci. Rev.*, pp.95-125.
- Dragicevic N. (2016). Model for erosion intensity and sediment production assessment based on erosion potential method modification. Doctoral Thesis, University of Rijeka, Faculty of Civil Engineering, p.192.
- Dragicevic N., Karleusa B., Ozanic N. (2017). Erosion Potential Method (Gavrilovic Method). Sensitivity Analysis. *Soil & Water Res.*, pp.51–59.
- Efthimiou N., Lykoudi E., Karavitis C. (2014). Soil erosion assessment using the RUSLE model and GIS. *European Water*, pp.15-30.
- Efthimiou N., Lykoudi E. (2016a). Soil erosion estimation using the EPM model. *Bulletin of the Geological Society of Greece, Proceedings of the 14th International Congress*, Thessaloniki, pp.305-314.
- Efthimiou N., Likoudi E., Panagoulia D., Karavitis C. (2016b). Assessment of soil susceptibility to erosion using the EPM and RUSLE models: the case of Venetikos river catchment. *Global NEST Journal*, pp.164-179.
- Flambouris K. (2008). Research of the effect of R factor in RUSLE method. Doctoral Thesis, Aristotle University of Thessaloniki, Department of Civil Engineering, p.181.
- Gavrilovic S. (1988). The Use of an Empirical Method (Erosion Potential Method) for Calculating Sediment Production and Transportation in unstudied or Torrential Streams, In White, W.R. (Ed.), *International Conference on River Regime*, Wiley, New York, pp.411-422.
- Kouli M., Soupios P., Vallianatos F. (2009). Soil erosion prediction using the Revised Universal Soil Loss Equation (RUSLE) in a GIS framework, Chania, Northwestern Crete, Greece. *Environmental Geology*, pp.483-497.
- Lappas I. (2018). Applied hydrogeological research in coastal aquifers. Case study of the coastal part of Atalanti region, Prefecture of Fthiotida. PhD Thesis, School of Mining and Metallurgical Engineering,



- National and Technical University of Athens, p.487.
- Maratos G., Rigopoulos K., Athanasiou A. (1965). Geological maps of Atalanti and Livanatessheets, scale 1:50.000, Institute of Subsurface Geological Research.
- McCool K., Foster R., Weesies A. (1997). Slope-length and steepness factors (LS). In *Predicting Soil Erosion by Water: A Guide to Conservation Planning with the Revised Universal Soil Loss Equation (RUSLE)*. *USDA Agriculture Handbook* No. 703, Chapter 4. Washington, DC: USDA.
- Mitasova H., Mitas L. (2001). Multiscale soil erosion simulations for land use management. In *Landscape erosion and landscape evolution modeling*, Harmon R. and Doe W. eds., Kluwer Academic/Plenum Publishers, pp.321-347.
- Montgomery R. (2007). Soil erosion and agricultural sustainability. *Proceedings of the National Academy of Sciences of the United States of America*, pp.13268-13272.
- Oikonomidis D., Lazos I. (2014). Estimation of soil erosion rate by the use of Remote sensing, GIS and precipitation data. Case study: Orestis (Kastoria) lake watershed, Northern Greece. *10th International Hydrogeological Congress of Congress of Greece*, Thessaloniki, pp.577-586.
- Panagos P., Borrelli P., Poesen J., Ballabio C., Lugato E., Meusburger K., Montanarella L., Alewell C. (2015a). The new assessment of soil loss by water erosion in Europe. *Environ. Sci. Policy*, pp.438-447.
- Panagos P., Ballabio C., Borrelli P., Meusburger K., Klik A. (2015b). Rainfall erosivity in Europe. *Science of Total Environment*, pp.801-814.
- Panagos P., Borrelli P., Meusburger C., Alewell C., Lugato E., Montanarella L., (2015c). Estimating the soil erosion cover-management factor at European scale. *Land Use Policy*, pp.38-50.
- Panagos P., Borrelli P., Meusburger K. (2015d). A new European slope length and steepness factor (LS-Factor) for modeling soil erosion by water. *Geosciences*, pp.117-126.
- Panagos P., Borrelli P., Meusburger K., Van der Zanden H., Poesen J., Alewell C. (2015e). Modelling the effect of support practices (P-factor) on the reduction of soil erosion by water at European Scale. *Environmental Science & Policy*, pp.23-34.
- Panagos P., Ballabio C., Meusburger K., Spinoni J., Alewell C., Borrelli P. (2017). Global rainfall erosivity assessment based on high-temporal resolution rainfall records. *Sci. Rep.* pp.251-262.
- Pham T., Degener J., Kappas M. (2018). Integrated universal soil loss equation (USLE) and Geographical Information System (GIS) for soil erosion estimation in A Sap basin: Central Vietnam. *International Soil and Water Conservation Research*, pp.99-110.
- Renard K., Foster G., Weesies G., Porter J. (1991). RUSLE: revised universal soil loss equation. *Journal of Soil and Water Conservation*, pp.30-33.
- Renard K., Freimund J. (1994). Using monthly precipitation data to estimate the R factor in the revised USLE. *Journal of Hydrology*, pp.287-306.
- Renard K., Foster G., Weesies G., McDool D., Yoder D. (1997). *Predicting Soil Erosion by Water: A Guide to Conservation Planning with the Revised Universal Soil Loss Equation (RUSLE)*. Agricultural Handbook US Department of Agriculture, p.703.
- Renfro W. (1975). Use of Erosion Equations and Sediment Delivery Ratios for Predicting Sediment Yield. In *Present and Prospective Technology for Predicting Sediment Yield and Sources*, U.S. Department of Agriculture (USDA).
- Sigalos G., Loukaidi V., Dassaklis S., Alexouli-Livaditi A. (2010). Assessment of the quantity of the material transported downstream of Sperchios river, Central Greece. *Bulletin of the Geological Society of Greece, Proceedings of the 12th International Congress*, pp.737-745.
- Silva R., Santos C., Silva A. (2014). Predicting soil erosion and sediment yield in the Tapacura catchment, Brazil. *Journal of Urban and Environmental Engineering*, pp.75-82.
- Stefanidis S., Stathis D. (2018). Effect of Climate Change on Soil Erosion in a Mountainous Mediterranean Catchment (Central Pindus, Greece). *Water*, 1469.
- Vahaviolos Th. (2014). Soil erosion, sediment yield and reservoirs deposits estimation from empirical methods based on rainfall effect. Master's Thesis, National and Technical University of Athens, p.195.
- Van der Knijff M., Jones A., Montanarella L. (2000). Soil erosion risk assessment in Europe. European Soil Bureau. European Commission, JRC Scientific and Technical Report, EUR 19044 EN, p.58.
- Vanoni A. (1975). Sedimentation Engineering. In *Manuals and Reports on Engineering Practices*, ASCE,



New York.

Wischmeier H., Smith D. (1978). Predicting Rainfall Erosion Losses. A Guide to Conservation Planning. Agriculture Handbook No. 537, U.S. Department of Agriculture, Washington, U.S.A.

Xanthakis M., Minetos P., Lisitsa G., Kamari G. (2017). Numerical modelling of soil erosion in Cephalonia, Greece using geographical information systems and the revised soil loss equation (RUSLE). *18<sup>th</sup> Pan-Hellenic Forestry Conference & International Workshop*.

Yasoglou N. (2004). Soil Associations Map of Greece. Greek National Committee for Combating Desertification, Agricultural University of Athens.

Zarris D., Lykoudi E., Panagoulia D. (2012). Sediment yield assessment in Greece. *International Conference Sediment Transport Modeling in Hydrological Watersheds and Rivers*, Turkey.